Journal of Applied Polymer Science

# Improved Thermomechanical Properties of Carbon Fiber Reinforced Epoxy Composite Using Amino Functionalized XDCNT

**Mohammad K. Hossain,[1] Md Mahmudur R. Chowdhury,[1] Mahmud B. Salam,[1] Johnathan Malone,[1] Mahesh V. Hosur,[2] Shaik Jeelani,[2] Nydeia W. Bolden[3]**

[1]Department of Mechanical Engineering, Tuskegee University, Tuskegee, Alabama 36088

[2]Department of Materials Science and Engineering, Tuskegee University, Tuskegee, Alabama 36088

[3]Air Force Research Laboratory Munitions Directorate, Eglin AFB, Florida 32542

Correspondence to: M. K. Hossain (E-mail: hossainm@mytu.tuskegee.edu)

**ABSTRACT:** Carbon fiber-reinforced epoxy composites (CFEC) are fabricated infusing up to 0.40 wt % amino-functionalized XD-grade carbon nanotubes (XDCNT) using the compression molding process. Interlaminar shear strength (ILSS) and thermomechanical properties of these composites are evaluated through short beam shear and dynamic–mechanical thermal analysis tests. XDCNTs are infused into Epon 862 resin using a mechanical stirrer followed by sonication. After the sonication, the mixture was placed in a three roll milling processor for three successive cycles at 140 rpm for uniform dispersion of CNTs. Epikure W curing agent was then added to the resin using a high-speed mechanical stirrer. Finally, the fiber was reinforced with the modified resin using the compressive mold. ILSS was observed to increase by 22% at 0.3 wt % XDCNT loading. Thermal properties, including storage modulus, glass transition temperature, and crosslink density demonstrated linear enhancement up to the 0.3 wt % XDCNT loading. Scanning electron microscopy revealed better interfacial bonding in the CNT-loaded CFEC. © 2014 Wiley Periodicals, Inc. J. Appl. Polym. Sci. **2014**, *131*, 40709.

**KEYWORDS:** composites; crosslinking; manufacturing; nanoparticles; nanowires and nanocrystals; thermal properties

Received 8 January 2014; accepted 10 March 2014

**DOI: 10.1002/app.40709**

## INTRODUCTION

In a fiber reinforced composite, the matrix is the first to fail upon loading because it is the weakest constituent. Hence, the improvement of matrix properties is expected to enhance the overall performance of composites. In the last two decades, researchers have successfully enhanced the matrix properties by incorporating various nanoparticles into epoxy resin and its fiber-reinforced composites.[1–3] Carbon nanotubes (CNTs) have been proven to be a potential candidate for matrix modification because of its exceptional strength and stiffness, high specific surface area, and high aspect ratio. The higher specific surface area of CNTs facilitates a strong interface for better stress transfer from the matrix to the fiber by bridging effect. However, CNTs excessive agglomeration tendency can produce unwanted stress concentrations that may act as a precursor for failure during loading. Hence, the uniform dispersion of CNTs is considered to be the most important parameter in fabricating reinforced composites. Chemical functionalization of the CNT surface was found to further improve the interfacial interaction between CNTs and matrix as well as dispersion of CNTs into the matrix.[4–6] It had been observed that amino functionalization of CNTs enhanced the dispersibility in the epoxy matrix.[7] Moreover, multiwalled carbon nanotubes (MWCNTs) exhibited better dispersion in polymer than the single- or double-walled CNTs (SWCNT or DWCNT).[8] In order to have sufficient stress transfer from the matrix to the CNTs and to efficiently exploit the potential of CNTs as structural reinforcement, a strong interfacial adhesion between the CNTs and polymer is desired. The increase in interfacial adhesion between CNTs and matrix can be improved by functionalizing the CNTs.[4–6]

There is a growing demand for low cost materials in the microelectronic devices and civil infrastructure industry.[9] With this rationale, there is extensive research in progress on polymer-based nanocomposites to improve electrical, thermal, mechanical, and magnetic properties. However, the cost comparison with cheaper reinforcement particulates does not proportionately favor the use of nanotubes. The electrical XD-grade CNTs (XDCNTs) consist of SWCNTs and DWCNTs along with carbon black and metallic impurities.[10] XDCNT ($50/g) which is produced by a high yielding process is cheaper than the SWCNT ($350–$1000/g). However, the difference in mechanical properties of nanocomposites consisting of these nanofillers is studied rarely. Okoro et al.[11] studied effects of XDCNTs on the mechanical properties of Epon 862/W nanocomposite. They reported

improved flexural properties due to the addition of CNTs in the resin matrix while the storage modulus remained unchanged in the glassy region. A slight increase in storage modulus was found near the glass transition temperature region. Glass transition temperature remained unchanged upon addition of CNTs because CNTs have minimal effect on restricting polymer chain movement at higher temperature.

Dynamic mechanical thermal analysis (DMTA) was performed to observe stiffness behavior of laminates as a function of temperature and to assess the effect of CNTs on thermo-mechanical performance. In general, storage modulus, loss modulus, and glass transition temperature of laminates are expected to increase upon loading of MWCNTs. This behavior can be attributed to the improved dispersion and interaction between the CNTs and epoxy due to the formation of covalent bonds between them. The interfacial interaction reduces the mobility of the epoxy polymer chain around the nanotubes which leads to increase in elastic properties in final composites below the rubbery region. The loss modulus of composites is also expected to increase with the addition of CNTs. Loss modulus of composites indicates the energy used to deform the material. This energy is dissipated into heat and can be used as a measurement of viscous component or unrecoverable oscillation energy dissipated per cycle. Better dispersed nanotubes must dissipate energy due to resistance against viscoelastic deformation of the surrounding matrix. It was reported that covalent bond between amino-functionalized CNTs and epoxy improve the efficiency of load transfer from matrix to fillers resulting in an increase in loss modulus due to more energy dissipation in composites.[12] It was found that the combination of high speed shear mixing and sonication is the best dispersion technique for infusing MWCNTs (0.1–0.4 wt %) in Epon 862 resin with improved thermomechanical properties.[3] Flexural strength and modulus were improved by 28 and 12%, respectively, for 0.3 wt % CNT loading compared to those in the control system. An increase in dynamic mechanical properties up to 0.3 wt % loading of CNTs with the improvement of around 90% in storage modulus and 22°C in glass transition temperature ($T_g$) compared to the reference one was also reported.[3] The effect of amino functionalized MWCNTs on the thermal and mechanical properties of E-glass/epoxy laminated composite cured in the compression hot press was studied.[13] Improvement in flexural and ILSS due to the addition of 0.3 wt % MWCNTs was documented. From the dynamic mechanical analysis (DMA), it was observed that CNTs significantly increase laminate's useful operating temperature range, its storage modulus, loss modulus. However, $T_g$ was deteriorated due to the incorporation of CNTs. Temperature sensitivity of these thermal properties and a good correlation among them were also observed.

In the last two decades, many researchers have worked to improve the ILSS of fiber reinforced polymer composites (FRPC) by incorporating nanoparticles.[14–18] Conventional manufacturing process of FRPC does not make the reinforcing fiber in the thickness direction strong enough to carry a large transverse load.[14] If nanoparticles can be arranged in the thickness direction, it will enhance the ILSS by transferring load from matrix to fiber. Fan et al.[19] implemented a novel injection and double vacuum assisted resin transfer molding (IDVARTM) method for laminate fabrication. This method was found effective to distribute oxidized MWCNTs between the layers up to 2 wt % uniformly. It was found that an addition of 2 wt % oxidized MWCNTs into glass fiber reinforced polymer (GFRP) composite increased the ILSS by 33%. The effect of MWCNTs, aliphatic diluents butyl glycidyl either (BGE), and the optimum simultaneous addition of these two into GFRP composites was investigated.[20] It was demonstrated that the simultaneous addition of 0.5 wt % MWCNTs and 10 parts BGE per hundred parts of resin (phr) has led to the highest ILSS with an increase of 25.4% compared to the control system. A high shear mixing process for dispersing the amino-functionalized DWCNTs into epoxy was used and nanophased glass fiber reinforced epoxy polymer composites by resin transfer molding (RTM) process was produced.[18] An improvement of 19% was obtained in ILSS due to the addition of 0.3 wt % DWCNT–$NH_2$ in the composite. Wichmann et al.[21] also found 16% enhancement in ILSS properties at 0.3 wt % of functionalized DWCNTs loading. The incorporation of 0.25 wt % of MWCNTs in carbon fiber reinforced epoxy composites manufactured by the vacuum assisted resin transfer molding (VARTM) method enhanced ILSS by 27%.[22]

In this study, amino functionalized XDCNTs were dispersed with a combination of sonication and the three roll mixing process. Finally, conventional and nanophased carbon fiber/epoxy composites were manufactured using the compression molding process. SBS and DMTA tests were performed to investigate the effect of XDCNTs on the mechanical and thermal properties of carbon fiber/epoxy composites. In addition, the effect of doping of XDCNTs into the matrix and fiber/matrix adhesion was investigated using SEM through the fracture morphology study. Resultant outcomes containing different wt % of CNT loadings were then compared with those of the conventional carbon fiber/epoxy composite.

SBS test results exhibit that the incorporation of XDCNTs into the composite increased the ILSS up to 22% at 0.3 wt % CNTs loading. DMTA test results in terms of storage modulus, glass transition temperature, and crosslink density demonstrated linear enhancement up to the 0.3 wt % XDCNTs-loaded samples. Better dispersion and alignment of XDCNTs facilitated more crosslinking sites, whereas, the reaction between functional groups (–$NH_2$) of XDCNTs with epoxide groups of resin and silanes of fiber surfaces improved the crosslinking and thereby ILSS properties of carbon/epoxy composites. Further, fracture morphology studied by scanning electron microscopy (SEM) revealed better interfacial bonding in the CNT-loaded CFEC.

## EXPERIMENTAL

### Materials

The matrix used in this study is a two part system. Part A is Epon 862 (Diglycidyl Ether of Bisphenol F), which is a low viscosity liquid epoxy resin manufactured using Bisphenol F and epichlorohydrin, and Part B is Epicure W, an aromatic diamine used as a curing agent of epoxy resin, obtained from Miller Stephenson Chemical Company, Danbury, CT. 8-harness satin weave carbon fabric purchased from US composites was used as reinforcement to fabricate laminates using the compression hot

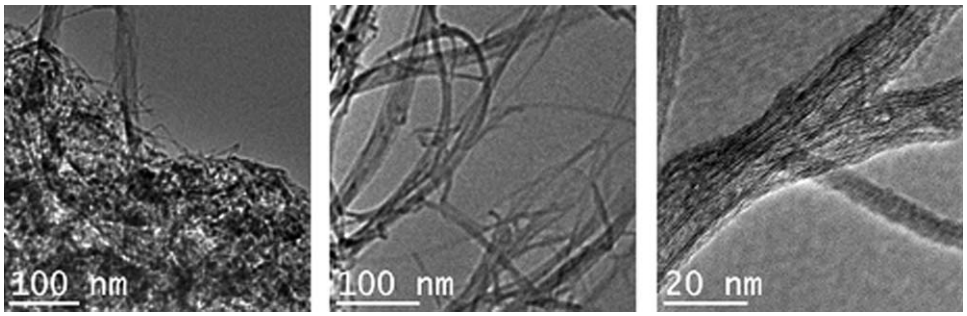


**Figure 1.** TEM micrographs of raw XD-CNTs.

press technique. XD-grade CNTs functionalized with amine groups ($NH_2$–XDCNTs) was received from Unidym, Houston. The XDCNTs consist of a mixture of SWCNT, DWCNT, and MWCNT, along with carbon black and metallic impurities. These CNTs had an average diameter of 9.5 nm and an average length of less than 1 μm. Concentration of functional groups was less than 4%. The transmission electron micrographs (TEM) of as-received carbon nanotubes at different magnifications are shown in Figure 1. These XDCNTs have applications for improving electrical conductivity in amorphous materials. The XDCNTs were covalent functionalized by amine ($–NH_2$) to achieve the required exfoliation and dispersion.

### Manufacturing Process

**Resin Preparation.** At first, a precalculated amount of amino functionalized XDCNTs (0.15, 0.3, or 0.4 wt %) were mechanically mixed with epoxy resin Part A by a mechanical stirrer for 4–5 min. The mixture was then put into a sonicator for 1 h at 35% amplitude and 40 s on/20s off cycle pulse mode. To avoid premature polymerization, this mixture was drowned thoroughly in a cooling bath. The sonicated mixture was then passed through the three rollers to further improve the dispersion of XD-CNTs. In this process, CNTs are further de-agglomerated and uniformly dispersed in resin by the induction of a high shear force in the mixture. The gap space was incrementally reduced from 20 to 5 $\mu$m between the rolls and multiple passes were used to induce a high shear force in the mixture. In all passes, the speed ratio of the three rollers was 1:3:9 with a maximum speed of 140 rpm. The XDCNT/epoxy mixture was then mixed with the curing agent Epikure W using a mechanical mixer according to the stoichometric ratio (Part A: Part B = 100:26.4). The mixture was then placed in a vacuum oven at 70°C for 30 min to ensure the complete removal of entrapped bubbles, and thus reduce the chance of void formation.

**Composite Fabrication.** Both conventional and nanophased carbon fiber-reinforced epoxy composites were fabricated by employing a combination of hand lay-up and compression hot press techniques. Compression molding uses high-pressure to manufacture complex and high strength fiber-reinforced composites in large volumes at a fast production rate. The main advantages of this fabrication method in the area of composites are: (1) low cost, (2) fast setup time, (3) capability of producing large and complex components, (4) high volume production, (5) dimensional control and stability, (6) good surface finish, (7) little material waste, (8) ability to use unidirectional tapes, woven fabrics, randomly orientated fiber mat or chopped strand, (9) ability to add inserts and rib stiffeners, and (10) fewer knit lines and less fiber-length degradation.[23]

Carbon woven fabrics were properly stacked into eleven layers while maintaining their parallel orientation. Modified epoxy resin was smeared uniformly on each fabric layer using a wooden roller and the laminates were consolidated by applying a 16 kips (71.12 kN) force in a hot press. The complete composite fabrication procedure is presented in Figure 2. Two curing cycles were used to cure the laminate under the hot press according to the manufacturer's suggestion at: (1) 121°C for 2 h and (2) 177°C for 2 h, respectively. After completion of the curing cycles, the laminate was allowed to cool down slowly to avoid any unwanted shrinkage. Finally, the cured laminate was taken out from the hot press and kept at 177°C for 2 h for postcuring.

### Material Characterization

**Matrix Digestion Test.** A matrix digestion test was conducted according to the ASTM D 3171-99 standard to estimate the fiber volume fraction and void content of carbon/XD-CNT/epoxy laminated composites. Samples with a dimension of 30 mm × 30 mm × 2 mm were cut from three randomly selected locations of the laminates and weighed precisely. Each sample was then immersed into a bath of 80% concentrated nitric acid ($HNO_3$) maintained at 70°C for about 5 h. After 5 h, matrix resin was digested completely by nitric acid only leaving out the carbon fibers. The fibers were then taken out from nitric acid and washed with distilled water and acetone repeatedly. Fibers were then dried in an oven maintained at 100°C for about an hour. After that fiber weight was measured. The following equations were used to calculate the fiber, matrix, and void volume fraction in the laminated composite:

$$\text{Fiber vol. fraction}, V_f = \frac{w/F}{w/C} \tag{1}$$

$$\text{Matrix vol. fraction}, V_m = \frac{(w-W)/M}{w/C} \tag{2}$$

$$\text{Void vol. fraction}, V_o = 1 - \left(V_f + V_m\right) \tag{3}$$

where, $W$ and $w$ are the weight of fiber in the composite and initial composite specimen, respectively; $F$, $M$, and $C$ are the density of fiber, matrix, and composite, respectively; and $V$ is the volume of composite. The composite density was measured by the New Classic MS Analytical Balance manufactured by Mettler Toledo.

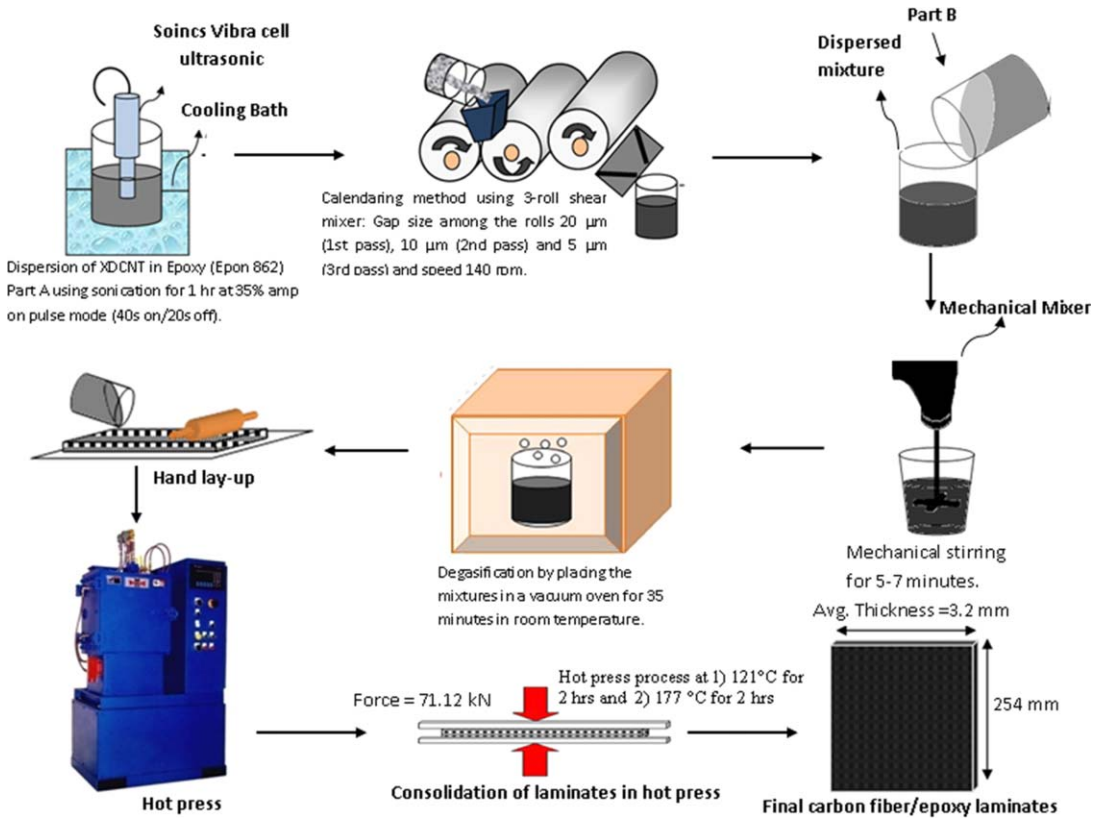


**Figure 2.** Schematic diagram of carbon fiber/epoxy nanocomposite fabrication. [Color figure can be viewed in the online issue, which is available at wileyonlinelibrary.com.]

**ILSS Characterization.** The apparent interlaminar shear strength (ILSS) of fabricated carbon/epoxy composites was determined using short beam shear (SBS) test as per the ASTM D-2344-00 standard. A minimum of six samples for each category were tested under three point bending configuration using the Zwick-Roell Z 2.5 testing unit at a crosshead speed of 1.2 mm/min. The specimen dimensions used for this test are 35 × 6.5 × 3.25 mm. The span length to depth ratio was 6 and the width was twice the thickness. The load was being applied at the center until the first failure occurred. The breaking load noted at this point was then used to calculate ILSS using the relation derived from classical beam theory:

$$\text{ILSS} = \frac{0.75P_b}{b \times h} \quad (4)$$

where '$P_b$' is the breaking load, '$b$' is the width of specimen and '$h$' is the thickness of specimen.

**Thermomechanical Characterization.** DMA was performed with a TA Instruments dynamic mechanical analyzer (Model Q800) according to the ASTM D4065-01 standard under a dual cantilever beam mode with a frequency of 1 Hz and amplitude of 15 µm. The temperature was ramped from 30 to 250°C at a rate of 5°C/min. A minimum of five samples of each category were tested.

TMA tests were carried out on a TA instruments thermo mechanical analyzer (Model Q400) operating in the expansion mode at a heating rate of 5°C/min from 30 to 250°C. Five samples of each type were tested, and the CTE for each of those samples was determined before the glass transition temperature.

**Fracture Morphology Study.** Fracture morphological properties of composite samples were evaluated through SEM study. Failed samples were cut through a cross section of the failed region. SEM analysis was carried out using a Zeiss EVO 50. SEM samples were positioned on a sample holder with a silver paint and coated with gold by a low vacuum sputtering machine prior to loading in the SEM to prevent charge build-up by the electrons absorbed by the specimen. A 20 kV accelerating voltage was applied to achieve desired magnification.

## RESULTS AND DISCUSSIONS

### Fiber and Void Volume Fractions of Carbon Fiber/Epoxy Composite

Table I shows average fiber volume fraction and void content in neat and 0.15–0.4 % XDCNT carbon fiber/epoxy composites. The average fiber volume fraction of the laminates was in the range of 70–72% and void fraction was in the range of 1.5–2.5%. Experimental fiber volume fraction in this study is higher than those obtained from theoretical calculation which is around 50%.[8] This is due to the weave pattern of carbon fabric which does not alleviate smooth infiltration of resin inside the fibers. Moreover, the applied compressive pressure during the hot press molding process was also responsible for the variation in fiber volume fraction. Higher compressive pressure is required to reduce void content. However, it ejects more resin

**Table I.** Physical Properties of Carbon/XDCNT/Epoxy Composites

| | Sample specification | | | |
|---|---|---|---|---|
| Properties | Neat | 0.15 wt % | 0.3 wt % | 0.4 wt % |
| Fiber volume fraction (%) | 71.56 ± 0.25 | 70.95 ± 0.66 | 71.22 ± 1.17 | 72.19 ± 0.41 |
| Void fraction (%) | 1.87 ± 0.39 | 2.27 ± 0.75 | 2.13 ± 0.48 | 2.45 ± 0.14 |
| Density (g/cm$^3$) | 1.592 ± 0.016 | 1.582 ± 0.022 | 1.584 ± 0.035 | 1.589 ± 0.018 |

from the laminate which, in turn increases the fiber fraction. From Table I, it can be observed that with increase of XDCNT loading, the void content also increases. It can be attributed mostly due to the increase of resin viscosity. The increased viscosity may obstruct the evacuation of entrapped bubbles and volatile impurities during epoxy resin processing. The presence of voids has a detrimental effect on the mechanical properties of carbon fiber/epoxy composite. On the other hand, addition of well dispersed CNTs improves the properties due to better interfacial interactions between modified epoxy and carbon fibers. Observed results in the current study are the net effects of these two opposing phenomena.

### Interlaminar Shear Strength (ILSS) Properties of CFEC

Short beam shear (SBS) test was performed on neat and nanophased CFEC to obtain their interlaminar shear strength (ILSS) which is a measurement of fiber-matrix binding strength. Generally in SBS test, failure occurs due to a combination of interlaminar shear cracking, microbuckling, indentation, and fiber rupture of the specimens.[19,24] Pure shear failure may not occur during SBS test. Hence, it is difficult to assure that the interlaminar shear failure will occur at the midplane.[8] Figure 3 shows the load vs. deflection curves of conventional and 0.15–0.4 wt % carbon/epoxy samples obtained from the SBS test. In load–displacement curves, a gradual rise up to the maximum load was observed followed by a sudden fall. This distinct failure behavior in these samples was predominantly due to interlaminar shear failure. This can be attributed to the fiber/matrix delamination or matrix cracking or in some cases due to the combination of both. Basically, a bending force was acting on the surface under the central loading zone. Therefore, this zone is subjected to compression and the samples may undergo localized buckling resulting in resin microcracking. From Figure 4, it can be seen that considering the low concentration of XDCNT loading the improvement in ILSS is significant. The ILSS was observed to be the highest in case of 0.3 wt % samples with 22% increase in comparison to control samples (Table II). Improved load transferring ability between epoxy matrix and nanotubes and more robust interfacial bonding between matrix and fiber are the conspicuous reasons that are responsible for enhancements in ILSS properties. Generally after mixing epoxy Part A and XDCNT–$NH_2$, the interfacial reaction takes place between amine functional groups of CNTs and epoxide groups of DGEBPF resin, which consists of ring opening reactions followed by a cross-linking reaction shown in Figure 5.[7] The cross-linking between amino groups of CNTs and epoxide group of resin might result in improved ILSS in 0.3 wt % loading through the possibility of effective stress transfer between epoxy and CNTs. As the XDCNTs are bridged by crosslinking, crack tips cannot break these when cracks propagate in nanocomposites through a CNT. The large volume of pulled nanotubes reduces the energy of the crack tips considerably, which in turn slows down the crack tips and forces the cracks to change their propagation line. This phenomenon makes crack initiation and propagation more difficult within the matrix and at matrix–fiber interface as compared to samples without CNTs.

Silanes, which are generally present on the surface of carbon fiber, may react with both epoxy systems and amine groups of XDCNTs. Silane treatment of carbon fibers was done by the manufacturer to make a durable bond between the fiber and

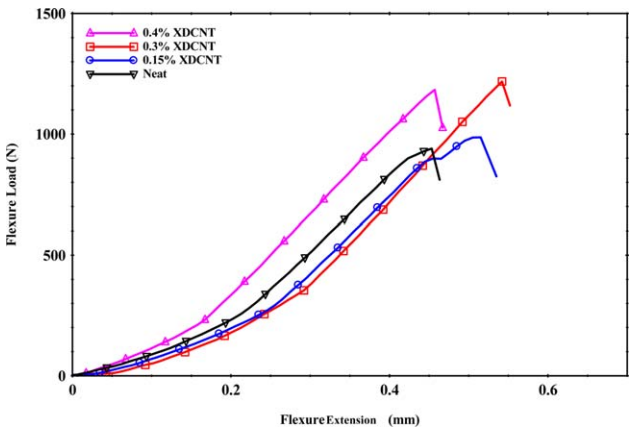


**Figure 3.** Load vs. deflection curve of carbon fiber/epoxy composites. [Color figure can be viewed in the online issue, which is available at wileyonlinelibrary.com.]

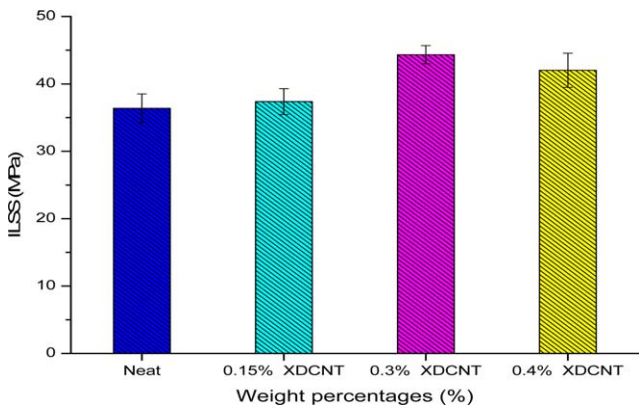


**Figure 4.** ILSS property at various XD-CNT concentration. [Color figure can be viewed in the online issue, which is available at wileyonlinelibrary.com.]

**Table II.** ILSS Properties of Carbon/XDCNT/Epoxy Composites

| Specimen number | ILSS (MPa) | | | |
|---|---|---|---|---|
| | Neat | 0.15 wt % | 0.3 wt % | 0.4 wt % |
| 1 | 37.90 | 40.07 | 42.52 | 38.3 |
| 2 | 37.39 | 38.56 | 46.22 | 42.36 |
| 3 | 34.76 | 35.4 | 44.42 | 39.67 |
| 4 | 38.38 | 36.02 | 43.78 | 43.88 |
| 5 | 33.55 | 36.79 | 44.68 | 42.96 |
| Average | 36.39 | 37.37 | 44.32 | 41.43 |
| Standard deviation | 2.117036 | 1.920018 | 1.349178 | 2.350676 |

matrix.[25] Once a silane is covalently bound to the fiber, a wide range of chemical reactions is possible with both epoxy systems and amine groups of XDCNTs. Silane consists of a generic chemical structure $R_{(4-n)}$–Si–$(R'X)_n$ $(n = 1, 2)$, where $R$ is alkoxy, $X$ represents an organofunctionality, and $R'$ is an alkyl bridge or alkyl spacer connecting the silicon atom and the organofunctionality.[26] This silicon-bearing monomer contains two types of reactive groups: (1) a hydrolysable group (Si–OR) that can condense with hydroxyl functionalities on the surface of fiber and (2) a functional group ($X$) which is compatible or capable of reacting with the matrix material.[27–29] Thus, the two functionalities allow silane to couple dissimilar materials together resulting in significant improvements in fiber–matrix bond strengths. The adsorbed silane usually exists as surface-tethered crosslinked network of varied thickness in real life applications. A three-dimensional interphase is created by interdiffusion and chemical reactions between the polymer matrix and silane layer resulting in an interpenetrating network (IPN) type of molecular architecture in the fiber–matrix interphase region.[30,31] The interfacial reaction takes place between primary amine of functionalized CNTs and epoxide groups of DGEBPF resin. The epoxide group of organosilane (3-glycidoxypropyltrimethoxy silane) might react with the secondary amine of functionalized XDCNTs. Hence, strong covalent bonds can be formed by this three-pronged chemical reaction shown in Figure 6. The covalent bond can increase the interfacial bonding between the matrix and the fiber, thus offering a resistance to the propagation of the crack. This better interfacial interaction can facilitate efficient stress transfer from a lower modulus matrix to a much higher modulus CNT to a higher modulus fiber resulting in an increase in ILSS.

### Dynamic Mechanical Analysis (DMA)

Various properties of laminated composites, such as storage modulus and tan$\delta$, which are dependent on temperature, were obtained by performing dynamic mechanical analysis. These properties characterize stored elastic energy and the energy dissipated during mechanical strain both of which are highly affected by fillers characteristics, i.e., geometry, weight fractions, dispersion state of fillers in matrix as well as adhesion between the reinforcements and matrix.[32] Figure 7 shows the temperature dependence of storage modulus in the range of 30–250°C.

(a) **Reaction of epoxide group (DGEBPF) with primary amine of functionalized XD-CNT**


(b) **Reaction of epoxide group (DGEBPF) with primary amine of functionalized XD-CNT**

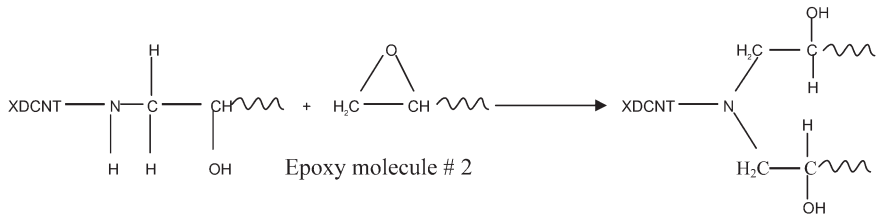


(c) **Cross-linking reaction between epoxy and XD-CNT**

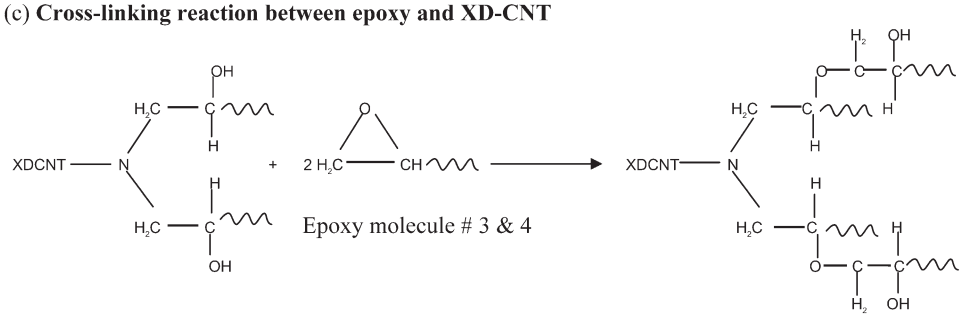


**Figure 5.** Schematic representation of interfacial reaction between DGEBPF (Part A) and XDCNT–$NH_2$.

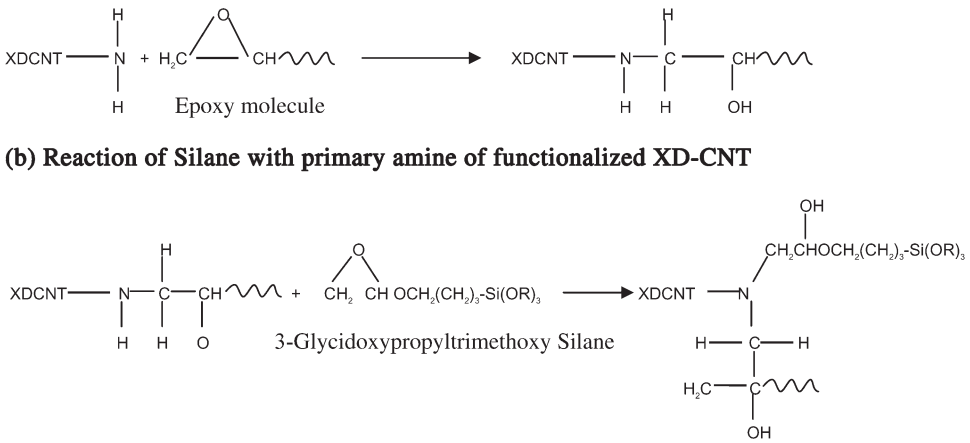


**Figure 6.** Schematic representation of interfacial reaction between DGEBPF (Part A), XDCNT–$NH_2$ and organosilane present on fiber.

For different laminates, storage modulus at 30°C has been presented in Table III. It can be seen that the addition of CNT concentration has resulted in significant improvement in storage modulus. Specifically, the storage modulus was improved by 17.22% with the addition of 0.3 wt % of XDCNT. This improvement is due to enhanced interaction between well dispersed CNTs and the matrix. More sites for XDCNT/polymer interaction have been provided by better dispersion of XDCNTs at 0.3 wt %. The formation of a strong covalent bond attributed to the presence of amino functional groups of XDCNT and its reaction with epoxy and silane. Hydrogen atoms in amine groups of DETA molecule (hardener) form self-crosslink with each other through reaction with the epoxide group of DGEBPF resin molecules in the case of the control epoxy sample. In case of nanophased samples (Figure 5), at first the interfacial reaction between amine functional groups of CNTs and epoxide groups of DGEBPF resin takes place by ring opening reaction after Epon 862 Part A and XDCNT–$NH_2$ have been mixed. This modified Part A establishes a strong covalent bond between epoxy and CNTs upon further mixing with Part B of epoxy resin and thereby crosslinking sites and interfacial bonding are boosted. The epoxy chain molecular motion around nanotubes has been abridged by the formation of covalent bond and the enhanced interaction. This abridgement may have resulted in a significant change of elastic and viscous properties in nanocomposites. However, at 0.4 wt % loading, the observed decrease in storage modulus can be attributed to increase of agglomeration of XDCNTs which reduces the crosslinking sites. Therefore, the storage modulus decreases as a result of increased molecular motion and movement of the chain. The covalent bond between epoxy and nanotubes is the primary factor in the improvement of thermomechanical properties. As in storage modulus, loss modulus was also increased up to 0.3 wt % CNTs compared to the control sample (Figure 8). The storage modulus drops sharply above 120°C because of the easier movement of the polymer chain. The temperature region where such a behavior is displayed is called the glass transition temperature ($T_g$). The operating region of the composite lies below $T_g$. The tan$\delta$ vs. temperature relationship in Figure 9 demonstrates the effect of nanotube concentration on damping properties of laminated composite. The addition of small amount of CNTs up to 0.3 wt % is observed to increase $T_g$ slightly. The $T_g$ of control system is about 155°C while it is observed to be 158 and 161°C, for 0.15 and 0.3 wt% XDCNTs reinforced composites, respectively (Figure 10). For the 4 wt % CNT-infused composite the $T_g$ is observed to be about the same as that of the control sample. The increase in $T_g$ in the polymeric system is predominantly affected by the amount and dispersion of CNTs, degree of crosslinking, and interfacial interaction.[33,34] When the CNTs are well dispersed the molecular motions are restricted and degree of crosslinking and interfacial interaction are improved. A positive shift of the curves in the tan$\delta$ vs. temperature plots is the indication of increase in $T_g$. For 0.4 wt % samples, interfacial adhesion between nanofiller and matrix is somewhat lower and molecular mobility is higher because of the presence of agglomerates. These effects have been indicated by the maximum decrease of tan$\delta$ peak for the 0.4 wt % CNT-loaded sample as

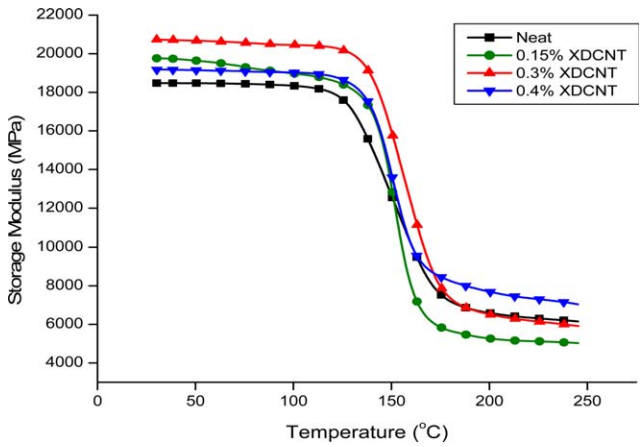


**Figure 7.** Temperature dependence of storage modulus for CFRP composites. [Color figure can be viewed in the online issue, which is available at wileyonlinelibrary.com.]

**Table III.** Thermomechanical Properties of Carbon/XDCNT/Epoxy Composites

| | Thermo-mechanical properties of carbon/XDCNT/epoxy nanocomposites | | | | | | | |
|---|---|---|---|---|---|---|---|---|
| Specimen category | Storage modulus (MPa) | Percentage change with respect to control | Loss modulus (MPa) | Percentage change with respect to control | Glass transition temperature (°C) | Percentage change with respect to control | CTE (μm/(m°C)) (before $T_g$) | Percentage change with respect to control |
| Neat | 18119 ± 249 | - | 1519 ± 16 | - | 155.7 ± 1.34 | - | 51.87 ± 2.53 | |
| 0.15 wt % | 19309 ± 292 | 6.57 | 1558 ± 21 | 2.57 | 158.43 ± 1.43 | 2.73 | 46.46 ± 1.85 | −10.43 |
| 0.3 wt % | 21239 ± 166 | 17.22 | 1736 ± 37 | 14.31 | 161.21 ± 2.38 | 5.51 | 32.4 ± 1.93 | −37.54 |
| 0.4 wt % | 19275 ± 364 | 6.38 | 1576 ± 50 | 3.75 | 155.99 ± 0.96 | 0.29 | 44.4 ± 2.41 | −14.4 |

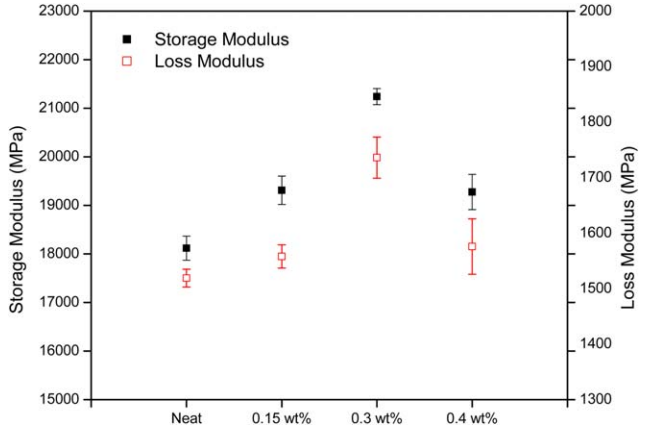


**Figure 8.** Variation in storage and loss modulus as a function of CNT content. [Color figure can be viewed in the online issue, which is available at wileyonlinelibrary.com.]

compared to the control one. Moreover, broader distribution of relaxation time is the byproduct of enhanced filler–matrix interaction, which interprets the significant widening of the tan$\delta$ peaks of composite sample with addition of CNTs. Relaxation of polymer chain can be disturbed by the nanotubes in their neighboring areas. However, nanotubes cannot disturb relaxation of polymer chains which are far away from them. Such variation in the nanotube concentration affects the formation of crosslinking and the relaxation behavior.[34,35]

### Coefficient of Thermal Expansion (CTE)

The coefficient of thermal expansion (CTE) is an important thermomechanical property of polymeric composites for engineering applications. Most of the polymeric materials have high CTE value which limits their applications. However, an incorporation of a small amount of nanoparticles as filler material in the polymeric matrix can significantly reduce the overall CTE of carbon/epoxy composites.[36,37] A low CTE value is most desirable to ensure good dimensional stability. In thermomechanical

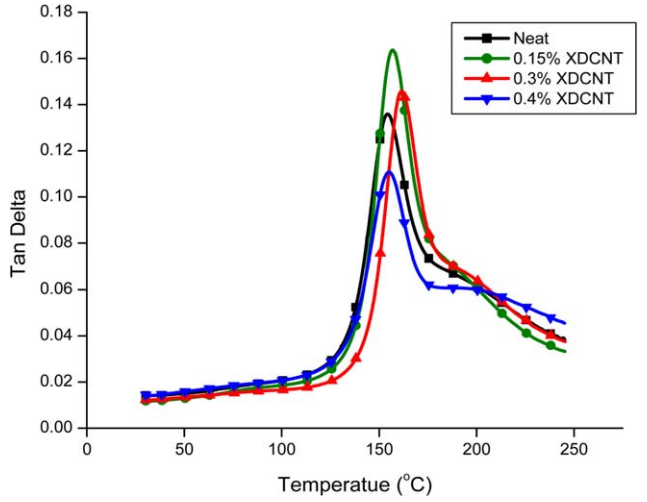


**Figure 9.** Temperature dependence of loss factor for CFRP composites. [Color figure can be viewed in the online issue, which is available at wileyonlinelibrary.com.]

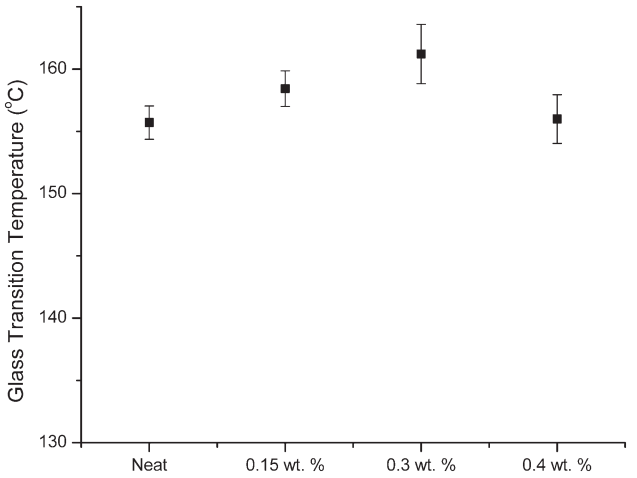


**Figure 10.** Variation in glass transition temperature as a function of CNT content.

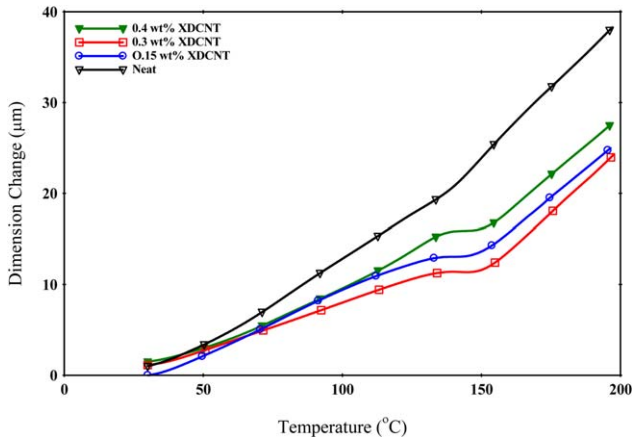


**Figure 11.** Dimension change with temperature for CFRP composites. [Color figure can be viewed in the online issue, which is available at wileyonlinelibrary.com.]

analysis, the dimensional change due to the temperature variation is usually measured in the thickness (transverse) direction of the sample. To measure the CTE, square specimens measuring 10–12 mm in length and 3–4 mm in thickness are subjected to a small load via a vertically adjustable quartz glass probe. The probe is integrated into an inductive position sensor. If the specimen expands or contracts due to heating and cooling, it moves the probe allowing the dimensional change to be measured, as a function of temperature.

The resin as a binding material typically exhibits a much higher CTE than that of the fiber. In general, the fiber is thermally as well as mechanically anisotropic. Hence, the CTE for FRP composites varies in the transverse as well as the perpendicular (longitudinal) directions depending on the types of fiber and resin, the fiber volume fraction, the fiber orientation, the void volume fraction, moisture effects, and resin viscoelasticity. Fiber reinforced polymeric (FRP) composites consist of unidirectional fibers or woven fabrics and there is no fiber in the transverse direction to support the load. The absence of transverse fibers/fabrics results in an extremely high CTE in the transverse direction as compared to that in the longitudinal direction. In essence, the transverse CTE is mainly due to the resin. On the other hand, the longitudinal CTE of the composite is very low and close to the CTE of the virgin fiber/fabric. This is attributed to the much higher Young's modulus of the fiber/fabric as compared to that of the matrix material.

The high strength (≈30 GPa) and elastic modulus (≈1 TPa),[38] and low CTE ($\alpha_{axial} \approx -1.5 \times 10^{-6}\ K^{-1}$, $\alpha_{transverse} \approx -0.15 \times 10^{-6}\ K^{-1}$)[34,39] combined with the high aspect ratio of the CNTs make them ideal candidates for nanoreinforcement in polymer matrix composites. Since CNTs have almost zero CTE, the addition of CNTs with polymer chain may end up with an overall reduction in CTE of composite.[40] The improvement in the dimensional stability in the transverse direction for the functionalized CNTs can be attributed to the uniform dispersion of the CNTs throughout the matrix, and the ability of the functional groups to form covalent bonds with the matrix as well as enhancement in the crosslinking density during the curing process of the matrix. On the other hand, CNTs are expected to have very little influence on the CTE in the longitudinal direction due to the fiber being the dominant load-bearing material in this direction. Hence, CNTs are expected to be dominant in determining the shrinkage or expansion in the transverse direction of the composites.[39,41]

Figure 11 presents the change in sample dimension in transverse direction as a function of temperature. Figure 12 compares the CTE value of control, 0.15, 0.3, and 0.4 wt % XDCNTs reinforced laminated composite in the temperature range of 30–100°C, which are below the glass transition temperature. The data are also presented in Table III. The average coefficient of thermal expansion of the control sample was found to be 51.87 ppm/°C. The addition of 0.3 wt % nanotubes reduced this value to 32.4 ppm/°C which represents a decrease of 37.54%. The CTE values of 0.15 and 0.4 wt % samples follow the trend seen earlier, where the 0.15 wt % sample lowers the CTE value slightly (10.43%) and the 0.4 wt % sample lowers the CTE value by 14.40%). The improved dispersion of CNTs in matrix facilitates to enhance interfacial reactions and forms covalent bond between them. This covalent bond induces different

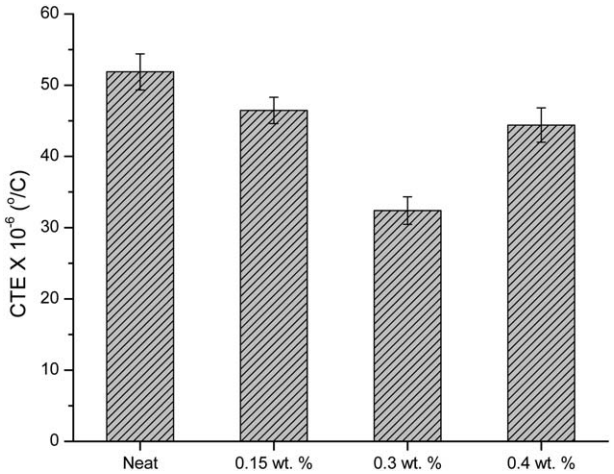


**Figure 12.** Comparison of CTE at different CNT content.

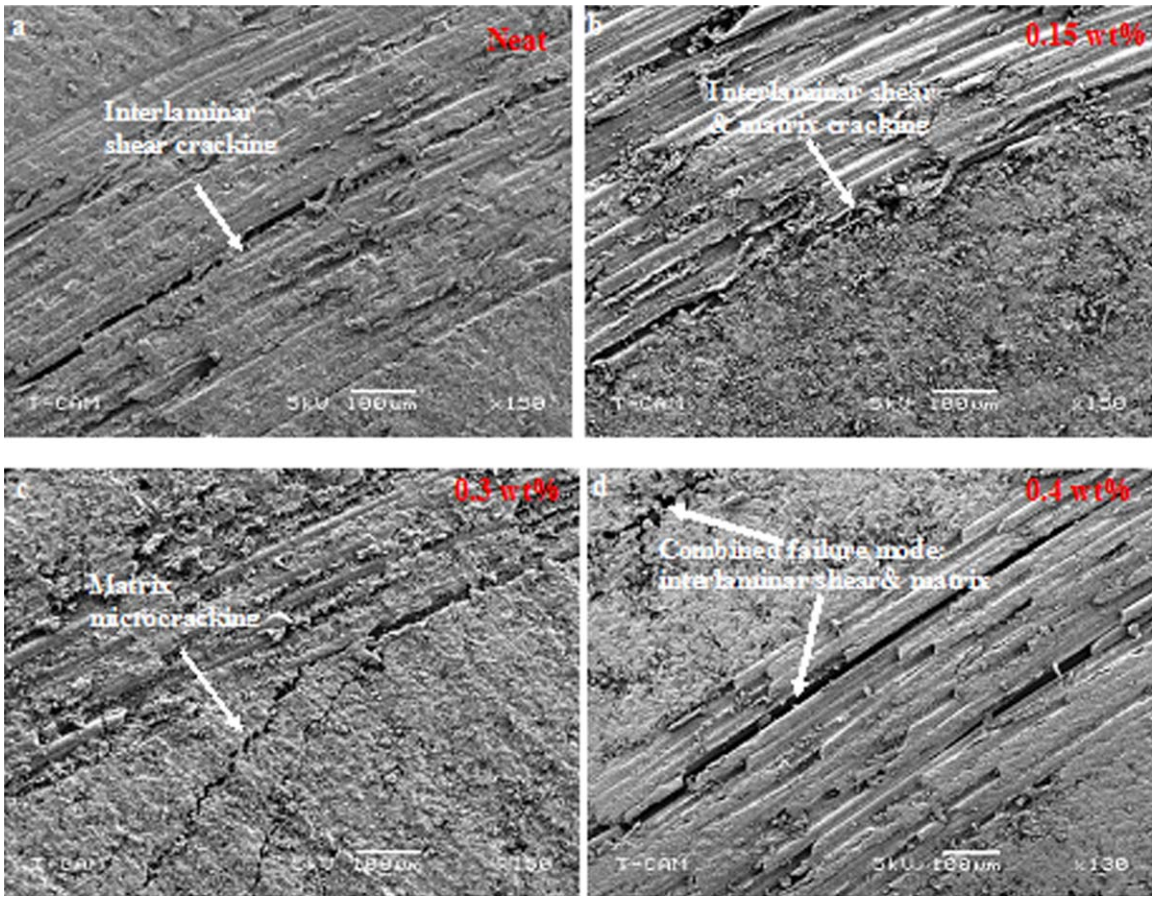


**Figure 13.** SEM micrographs SBS tested fractured surfaces: (a) neat, (b) 0.15 wt %, (c) 0.3 wt %, and (d) 0.4 wt % XDCNT infused CFRP composites. [Color figure can be viewed in the online issue, which is available at wileyonlinelibrary.com.]

crosslinking regions into the epoxy matrix. Generally after mixing epoxy Part A and $NH_2$–XDCNTs, the interfacial reaction takes place between amine functional groups of XDCNTs and epoxide groups of DGEBPF resin. Two ring opening reactions followed by a cross-linking reaction create interlocking structure in the resin blend those hindrances the mobility of polymer chains in the matrix system.[3] Thus, the reduction of CTE after addition of CNTs was due to its improved dispersion in the epoxy and the reduced segmental motion of the epoxy matrix.[42] Thus, improving the dimensional stability of the polymer matrix leads to improved dimensional stability in the resultant composite.[36] Moreover, well dispersed CNTs can align the

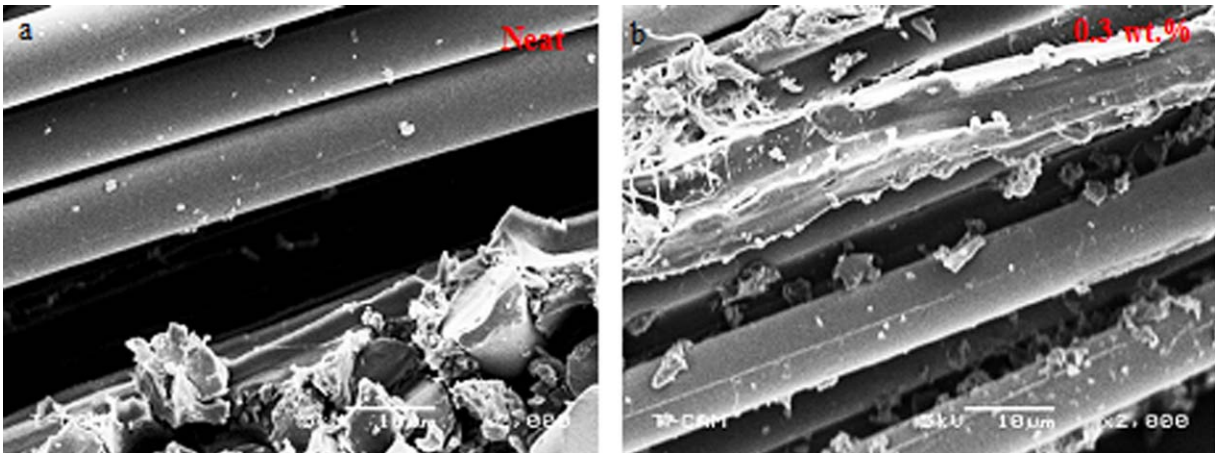


**Figure 14.** Interfacial bonding between fiber and matrix in (a) neat and (b) 0.3 wt % samples. [Color figure can be viewed in the online issue, which is available at wileyonlinelibrary.com.]

polymer chain along their axial direction, thus can easily get associated with the polymer molecule and prohibit its thermally induced movement resulting in a reduced CTE value.[39] The addition of 0.4 wt % CNTs resulted in slight increase in the CTE as compared to that of the 0.3 wt % sample, but still low in comparison with control system. This higher value of CTE can be demonstrated by the aggregates formed at a higher loading as explained in earlier sections.

**Fracture Morphology Study**

Results from the SEM study substantiate the quantitative results obtained through the SBS tests. The fracture morphology of conventional and nanophased carbon fiber/epoxy composites are presented in Figure 13. Interlaminar shear failure is clearly evident in the conventional composite [Figure 13(a)]. The failure mechanism in the 0.15 and 0.4 wt % nanophased composites is a combination of delamination and cracking at the matrix [Figure 13(b,d)]. However, the 0.3 wt% sample showed only matrix cracking [Figure 13(c)]. An increase in ILSS takes place when the failure occurs only in the matrix and not in the fiber–matrix interface during short beam shear test.

The fractured surface of nanophased CFEC demonstrates the presence of resin sticking to the fiber surface [Figure 14(b)], which is an indication of stronger interfacial bonding between the fiber and matrix. On the other hand, for the conventional CFEC shown in Figure 14(a), the fiber surface appears quite smooth and very little amount of resin adheres to the fiber. Moreover, the resin does not show any sign of protrusion into the surface of fibers [Figure 14(a)].These phenomena indicate a week interfacial bonding between the fiber and matrix. Moreover, the fracture surface of the CNT infused CFEC seems to be rougher compared to the conventional one. The rough surface suggests higher friction due to tougher bonding at the interface. The rough surface is also responsible for mechanical interlocking which enhances the interlaminar shear strength. Therefore, more energy is required to delaminate the composite. However, no such phenomenon was found in control samples. This phenomenon also explains that failure of conventional composite occurs due to the detachment of the resin from the fiber. When compared with the 0.3 wt % sample, the ILSS of 0.4 wt % sample was decreasing just like the DMA results. This decreasing might be attributed to the formation of excessive agglomeration as a result of the strong attractive forces among XDCNTs. At higher loading, CNTs get closer to each other in the matrix; hence their strong attractive forces might have led them to form agglomerates. These agglomerates can act as stress risers and also increase the free volume by creating voids in the matrix.[43,44] This phenomenon may contribute to premature matrix failure during loading which results in lower mechanical properties. At the same time, higher concentration of nanotubes in the resin may increase the resin viscosity significantly. High viscosity of the resin may cause poor wetting of the carbon fiber during laminate fabrication that in turn causes poor adhesion between the fiber and matrix.[45] Due to these factors, a reduction in the load transfer capability between CNTs and matrix systems may have occurred and hence the properties may have decreased at the 0.4 wt % loading.

## CONCLUSIONS

In this study, amino functionalized XDCNTs were infused as nanofillers in woven CFEC. The incorporation of XDCNTs at very low concentration (up to 0.3 wt %) enhanced the ILSS and thermomechanical properties of CFEC significantly. In this experimental investigation, the loading of 0.3 wt % XDCNTs was found to be optimum. The storage modulus was increased by 17.22 at 0.3 wt % loading in comparison to conventional CFEC. The glass transition temperature and loss modulus had also been improved slightly with the addition of XDCNTs. Significantly lower CTE was found in the 0.3 wt % XDCNT-infused CFEC compared to the control sample. The ILSS was also observed to have the highest value at 0.3 wt % loading due to better interfacial interaction and effective load transfer between $NH_2$–XDCNTs and epoxy resin. Scanning electron micrographs revealed that the functionalization of amino groups on XDCNTs surfaces promotes good adhesion between carbon fiber and epoxy matrix.

## ACKNOWLEDGMENTS

The authors acknowledge the Air Force Research Laboratory Munitions Directorate, Eglin AFB, FL 32542, USA (Grant No. FA8651-11-2-0004) and NSF-EPSCoR (Grant No. EPS-1158862) for their financial support to carry out this research work. DISTRIBUTION A. Approved for public release, distribution unlimited. (96ABW-2014-0072).

## REFERENCES

1. Farhana, P.; Zhou, Y.; Rangari, V.; Jeelani, S. *Mater. Sci. Eng.: Part A* **2005**, *405*, 246.
2. Mahfuz, H.; Adnan, A.; Rangari, V.; Jeelani, S.; Jang, B. Z. *Composit. Part A* **2004**, *35*, 519.
3. Zhou, Y.; Farhana, P.; Lewis, L.; Jeelani, S. *Mater. Sci. Eng.: A* **2007**, *452*, 657.
4. Yaping, Z.; Aibo, Z.; Quinghua, C.; Jiaoxia, Z.; Rongchang, N.; *Mater. Sci. Eng. A* **2006**, *145*, 435.
5. Xie, X.; Mai, Y. W.; Zhou, X. *Mater. Sci. Eng. A* **2005**, *49*, 89.
6. Sahoo, N. G.; Rana, S.; Cho, J. W.; Li, L. *Prog. Polym. Sci.* **2010**, *35*, 837.
7. Ma, P. C.; Mo, S. Y.; Tang, B. Z.; Kim, J. K. *Carbon* **2010**, *48*, 1824.
8. Mallick, P. K. Fiber Reinforced Composites; CRC Press: New York, **2007**.
9. Prasher, R. S.; Chang, J. Y.; Sauciuc, I.; Narasimhan, S.; Chau, D.; Chrysler, G.; Myers, A.; Prstic, S.; Hu, C. *Intel Technol. J.* **2005**, *9*, 285.
10. Tao, K.; Yang, S.; Grunlan, J. C.; Kim, Y. S.; Dang, B.; Deng, Y.; Thomas, R. L.; Wilson, B. L.; Wei, X. *J. Appl. Polym. Sci.* **2006**, *102*, 5248.
11. Okoro, C. U.; Hossain, M. K.; Hosur, M. V.; Jeelani, S. *J. Eng. Mater. Technol.* **2011**, *133*, 131.
12. Vlasveld, D. P. N.; Daud, W.; Bersee, H. E. N.; Picken, S. *J. Composit. Part A* **2007**, *38*, 730.

13. Rahman, M. M.; Zainuddin, S.; Hosur, M. V.; Malone, J. E.; Salam, M. B. A.; Kumar, A. S.; Jeelani, S. *Composit. Struct.* **2012**, *94*, 2397.
14. Rosselli, F.; Santare, M. H. *Composit. Part A* **1997**, *28*, 587.
15. Yokozeki, T.; Iwahori, Y.; Ishiwata, S. *Composit. Part A* **2006**, *38*, 917.
16. Siddiqui, N. A.; Woo, R. S. C.; Kim, J. K.; Leung, C. C. K.; Munir, A. *Composit. Part A* **2006**, *38*, 449.
17. Zhu, J.; Imam, A.; Crane, R.; Lozano, K.; Khabashesku, V.; Barrera, E. V. *Composit. Sci. Technol.* **2006**, *67*, 1509.
18. Gojny, F. H.; Wichmann, M. H. G.; Fiedler, B.; Bauhofer, W.; Schulte, K. *Composit. Part A* **2005**, *36*, 1525.
19. Fan, Z. H.; Santare, M. H.; Advani, S. G. *Composit. Part A* **2008**, *39*, 540.
20. Liu, Y.; Yang, J. P.; Xiao, H. M.; Qu, C. B.; Feng, Q. P.; Fu, S. Y.; Shindo, Y. *Composit. Part B* **2012**, *43*, 95.
21. Wichmann, M. H. G.; Sumfleth, J.; Gojny, F. H.; Quaresimin, M,; Fiedler, B.; Schulte, K. *Eng. Fract. Mech.* **2006**, *73*, 2346.
22. Beyakrova, E.; Thostenson, E. T.; Yu, A.; Kim, H.; Gao, J.; Tang, J.; Hahn, H. T.; Chou, T.-W.; Itkis, M. E.; Haddon, R. C. *Langmuir* **2007**, *23*, 3970.
23. Miracle, D. B.; Donaldson, S. L. ASM Handbook Volume 21: Composites; ASM International, **2001**; pp 516.
24. Subramaniyan, A. K.; Sun, C. T. *Composit. Part A* **2006**, *3*, 2257.
25. Kaynak, C.; Orgun, O.; Tincer, T. *Polym. Test.* **2005**, *24*, 455.
26. Xie, Y.; Hill, C. A. S; Xiao, Z.; Militz, H.; Mai, C. *Composit. Part A* **2010**, *41*, 806.
27. Tesoro, G.; Wu, Y. L. *J Adhes. Sci. Technol.* **1991**, *5*, 771.
28. Bayer, T; Eichhorn, K. J.; Grundke, K.; Jacobasch, H. *J. Macromol. Chem. Phys.* **1999**, *200*, 852.
29. Wang, D.; Jones, F. R. *Composit. Sci. Technol.* **1994**, *50*, 215.
30. Mader, E.; Pisanova, E. *Macromol. Symp.* **2001**, *163*, 189.
31. Dibenedetto, A. T. *Mater Sci. Eng. A* **2001**, *302*, 74.
32. Zhu, J.; Rodriguez-Macias, H.; Margrave, J. L.; Khabashesku, V. N.; Imam, A. M.; Lozano, K.; Barrera, E. V. *Adv. Funct. Mater.* **2004**, *14*, 643.
33. Abdallaa, M.; Dean, D.; Adibempe, D.; Nyairo E.; Robinson, P.; Thompson, G. *Polymer* **2007**, *48*, 5662.
34. Ganguly, S.; Roy, A. K.; Andersion, D. P. *Carbon* **2008**, *46*, 806.
35. Chowdhury, F. H.; Hosur, M. V.; Jeelani, S. *Mater. Sci. Eng. A* **2006**, *421*, 298.
36. Hossain, M. K.; Hossain, M. E.; Dewan, M. W.; Hosur, M.; Jeelani, S. *Composit. Part B* **2012**, *44*, 313.
37. Shokrieh, M. M.; Daneshvar, A.; Akbari, S. *Carbon* **2013**, *59*, 255.
38. Yu, M.-F.; Files, B. S.; Arepalli, S.; Ruoff, R. S. *Phys. Rev. Lett.* **2000**, *84*, 5552.
39. Lusti, H. R.; Gusev, A. A. *Model. Simulat. Mater. Sci. Eng.* **2004**, *12*, 107.
40. Chang, M. S. *J. Reinforc. Plast. Composit.* **2010**, *29*, 3593.
41. Zihong, L. Proceedings of the 50th Annual SAMPE Symposium, **2005**; p 2331.
42. Pramoda, K. P.; Linh, N. T. T.; Tang, P. S.; Tjiu, W. C.; Goh, S. H.; He, C. B. *Composit. Sci. Technol.* **2010**, *70*, 578.
43. Zhang, A. Y.; Li, D. H.; Zhang, D. X.; Lu, H. B.; Xiao, H. Y.; Jia, J. *Express. Polym. Lett.* **2011**, *5*, 708.
44. He, Q.; Yuan, T.; Yan, X.; Ding, D.; Wang, Q.; Luo, Z.; Shen, T. D.; Wei, S.; Cao, D.; Guo, Z. *Macromol. Chem. Phys.* **2014**, *215*, 327.
45. Song, Y. S.; Youn, J. R. *Carbon* **2005**, *43*, 1378.